Alexandria Engineering Journal (2016) 55, 357–368

HOSTED BY

Alexandria University

Alexandria Engineering Journal

www.elsevier.com/locate/aej
www.sciencedirect.com

ORIGINAL ARTICLE

Parameters estimation of squirrel-cage induction motors using ANN and ANFIS

Mehdi Ahmadi Jirdehi, Abbas Rezaei *

Electrical Engineering Department, Kermanshah University of Technology, Kermanshah, Iran

Received 9 July 2015; revised 20 January 2016; accepted 27 January 2016
Available online 12 February 2016

KEYWORDS

Parameters estimation;
Induction motor;
Squirrel-cage;
Artificial neural network;
Adaptive neuro-fuzzy inference system

Abstract In the transient behavior analysis of a squirrel-cage induction motor, the parameters of the single-cage and double-cage models are studied. These parameters are usually hard to obtain. This paper presents two new methods to predict the induction motor parameters in the single-cage and double-cage models based on artificial neural network (ANN) and adaptive neuro-fuzzy inference system (ANFIS). For this purpose, the experimental data (manufacturer data) of 20 induction motors with the different power are used. The experimental data are including of the starting torque and current, maximum torque, full load sleep, efficiency, rated active power and reactive power. The obtained results from the proposed ANN and ANFIS models are compared with each other and with the experimental data, which show a good agreement between the predicted values and the experimental data. But the proposed ANFIS model is more accurate than the proposed ANN model.

1. Introduction

Induction motors especially the squirrel-cage motors have the advantages such as less necessity to repair and control, higher reliability, more efficiency and low price and size. The induction motors can be considered as the industry's motive motor [1]. To study and simulate the induction motors' behaviors, the starting details and the transient state faults should be considered. Therefore, for this purpose the induction motor parameters should be estimated by high precision [2]. The parameters estimation of the induction motor is an important topic in the electric drive literatures because the controller performance depends on the accuracy of the motor parameters used by the control algorithm [3–5]. The squirrel-cage type induction motors are usually modeled with single-cage and double-cage models. The parameters of these models can be obtained by two methods [6]:

1. With the information of the full load test, the maximum torque and current [7–9].
2. With the information of the no-load test and the locker-rotor test.

Nowadays, the various methods have been presented to estimate the parameters in the induction motors by the researchers [8–11]. In one of these methods, the transient stator current has been used to identify the parameters of an electromechanical mode of the induction motor. In [12], a new

* Corresponding author.
E-mail addresses: m.ahmadi@kut.ac.ir (M.A. Jirdehi), unrezaei@yahoo.com, a.rezaee@kut.ac.ir (A. Rezaei).
Peer review under responsibility of Faculty of Engineering, Alexandria University.

http://dx.doi.org/10.1016/j.aej.2016.01.026

Table 1 Manufacturer data of induction motors ($U = 400$ V, $f = 50$ Hz).

P (KW)	Cosρ_{FL}	T_M/T_{FL}	T_{ST}/T_{FL}	I_{ST}/I_{FL}	ω_{FL} (r/min)	η_{FL}
500	0.87	2.7	2.3	6.5	992	0.966
400	0.82	2.6	2.1	6.5	742	0.962
355	0.87	2.7	2.2	6.8	1486	0.967
250	0.8	3	2.2	7.3	991	0.91
200	0.87	2.7	2.7	7	1488	0.962
160	0.86	2.7	2.4	7	1487	0.96
110	0.86	3	2	7.6	2982	0.955
90	0.86	2.7	2.2	6.8	1480	0.94
75	0.86	2.4	2.1	6.3	1482	0.947
45	0.81	2.3	2.1	6	740	0.92
37	0.86	3.1	2.5	7	1475	0.929
30	0.88	2.7	2.3	6	2940	0.91
19	0.84	3.2	2.7	6.9	1460	0.905
15	0.92	2.9	2.2	6.6	2910	0.904
11	0.9	3.1	2.2	7	2945	0.91
8	0.74	2.5	2.1	4.6	960	0.86
315	0.84	3	2	7.3	991	0.962
132	0.86	3	2.7	7.2	1486	0.955
55	0.82	2.4	2.2	6	738	0.931
22	0.77	2.9	2.8	5.5	975	0.908

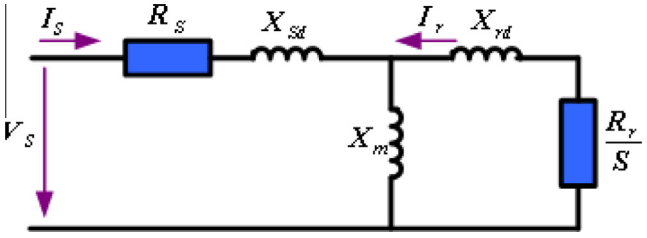

Figure 1 Single-cage induction motor steady state model.

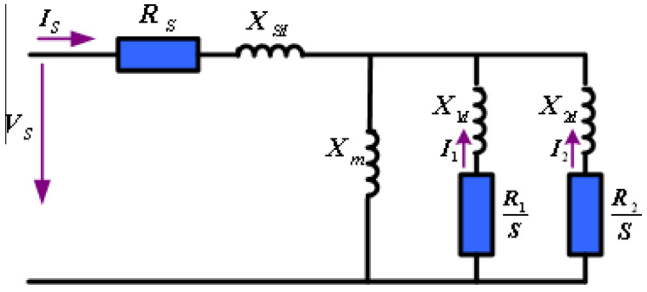

Figure 2 Double-cage induction motor steady state model.

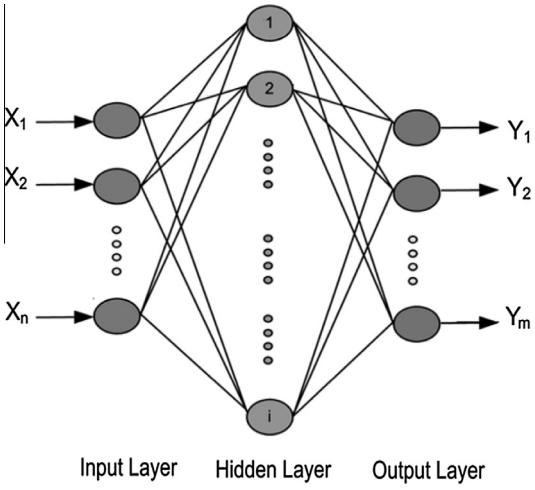

Figure 3 MLP structure.

method for determination of the steady-state equivalent circuit parameters of the wound-rotor induction motors has been presented using the experimental data from the starting transient measurements. Also, a new parameters determination method for squirrel-cage induction motors has been presented in [13] based on the instantaneous electrical power and the mechanical speed measured in a free acceleration test. In [14], the implementation of an adaptive neuro fuzzy inference system (ANFIS) technique to control the speed of the induction motor has been proposed and compared it with the PI and fuzzy controllers. In [15] a Takagi–Sugeno neuro-fuzzy inference system for direct torque and stator reactive power control has been applied to a doubly fed induction motor. In this case, the control variables (d-axis and q-axis rotor voltages) have been determined through a control system. More recently, authors have developed a two-step approach for parameters identification of induction motor form a nonlinear model including the magnetic saturation [16,17]. In [18], a new method to estimate the electrical parameters in a three-phase induction motor equivalent circuit has been presented using the genetic algorithm (GA). Also, in [19] the artificial bee colony (ABC) algorithm has been proposed and compared with the various recently methods for the parameters estimation of the induction motors. The shuffled frog-leaping algorithm has been introduced in [20] for the parameters estimation of a double-cage asynchronous machine using the standard manufacturer data. In these works, the induction motor parameters have been obtained from a relatively poor initial guess,

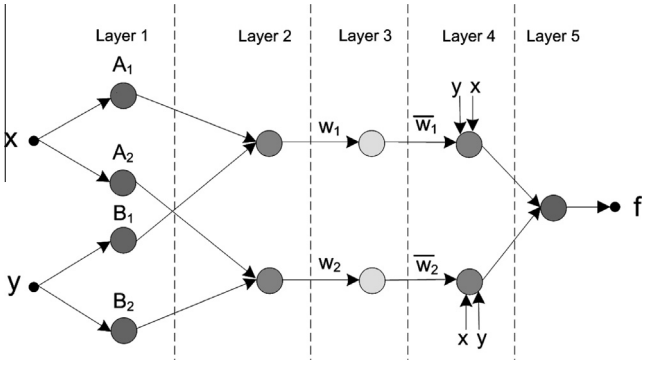

Figure 4 ANFIS structure.

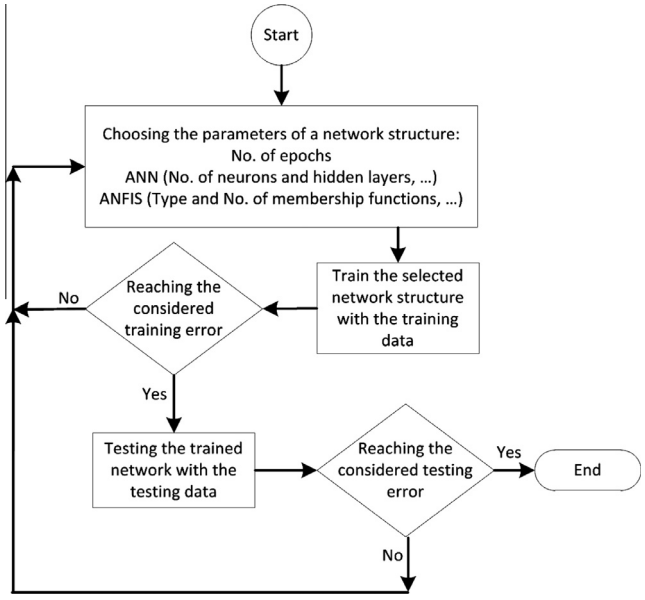

Figure 5 The ANFIS/ANN training process algorithm.

depending on the magnitude of the physical parameters, using a two-step strategy based on the nonlinear least-squares regression techniques. In this paper, a new method is proposed to estimate the parameters in the single-cage and double-cage models of the induction motors. The proposed method is based on artificial neural network (ANN) and ANFIS. For this purpose, the manufacturer data of 20 induction motors with the different synchronous speed (two poles to eight poles) and the line voltage of 400 V are used. Table 1 shows the manufacturer data of these induction motors (these data are obtained from the motor template), where the subscript "FL" refers to the full load, "M" refers to the point of the maximum torque, and "ST" refers to the starting point [9]. The rest of the paper is organized as follows: Section 2 summarizes the dynamic squirrel-cage induction motor model. The single-cage and double-cage induction motors formulation is presented in Section 3. In Section 4, the proposed ANN and ANFIS models for the parameters estimation of the induction motors are introduced. Finally, Section 5 describes the simulation results of the proposed methods and finally, the last section summarizes the conclusions of this study.

2. Dynamic model of squirrel-cage induction motors

In the various papers, the induction motors have been modeled as the single-cage model. This model is suitable for the motors with the winding rotor. This model is shown in Fig. 1.

For single-cage model, the steady state parameters in the equivalent circuit are the five electrical parameters R_S, R_r, X_m, X_{Sd} and X_{rd}. From these parameters, three parameters are the independent and the two other parameters are related to the independent parameters using Eq. (1):

$$R_S = K_r \cdot R_r, \quad X_{rd} = K_x \cdot X_{sd} \tag{1}$$

Two different methodologies have been followed to determine the single-cage model parameters. Method 1 obtains the parameters using the information of the full load point and the maximum torque. Method 2 determines the single-cage parameters with the information of the no-load test and the locker-rotor test. Both methods give significant errors, the first at the starting point and the second at the full load and the maximum torque points. The single-cage model does not represent the squirrel-cage induction motors well, and therefore the double-cage model must be used. For the caged rotor of the induction motor, the double-cage model is better than the single-cage model. Fig. 2 shows the double-cage model used to simulate induction motors' behaviors. The deep and narrow rotor bars have the torque-speed characteristics similar to those of a double-cage rotor.

The electrical parameters of the double-cage steady-state model are R_S, R_1, R_2, X_m, X_{Sd}, X_{1d} and X_{2d}. The parameters R_1 and X_{1d} represent the inner cage and the parameters R_2 and X_{2d} represent the outer cage. From these parameters, only five parameters are independent. Therefore, two relations are used:

$$\begin{aligned} R_S = \quad & K_r \cdot R_1, \quad X_{2d} = K_x \cdot X_{sd} \\ & R_2 > R_1, \quad X_{1d} > X_{2d} \end{aligned} \tag{2}$$

Finally, the motor parameters can be calculated using the following data:

$$P,\ Q,\ \frac{T_M}{T_{FL}},\ \frac{T_{ST}}{T_{FL}},\ \frac{I_{ST}}{I_{FL}} \tag{3}$$

where

P: Rated mechanical power
Q: Reactive power
T_M: Maximum torque
T_{ST}: Starting torque
T_{FL}: Full load torque
I_{ST}: Starting Current
I_{FL}: Full load Current

In the parameters estimation, $K_r = 0.5$ and $K_x = 1$ is usually a good suggestion for this purpose.

3. Single-cage and double-cage induction motors formulation

3.1. Single-cage model formulation

The determination of the single-cage parameters is interesting because its calculated values are a good starting guess for the double-cage problem.

Table 2 Specification of the best proposed ANN (MLP) models.

Specification	ANN model	
	Single-cage	Double-cage
Neural network	MLP	MLP
Number of hidden layer	2	2
Number of neurons in the input layer	7	7
Number of neurons in the first hidden layer	6	3
Number of neurons in the second hidden layer	4	5
Number of neurons in the output layer	4	6
Learning rate	0.5	0.5
Number of epochs	150	250
Adaption learning function	Trainlm	Trainlm
Activation function	Tansig	Tansig

For determination of the five single-cage parameters R_S, R_r, X_m, X_{Sd} and X_{rd}, the three pieces of manufacturer data P_{mFL}, Q_{FL} and T_M are used by solving the nonlinear functions in the form of $F(X) = 0$:

$$X = R_r,\ X_m,\ X_{sd} \quad F = f_1,\ f_2,\ f_3$$

$$\begin{cases} f_1(X) = P_{mFL} - Pm(S_{FL}) = 0 \\ f_2(X) = Q_{FL} - Q(S_{FL}) = 0 \\ f_3(X) = T_M - T(S_M) = 0 \end{cases} \tag{4}$$

$$R_S = K_r \cdot R_r, \quad X_{rd} = K_x \cdot X_{sd} \tag{5}$$

It is important to impose that all of the variables are always positive, which means the considering inequality restrictions $K_r > 0$ and $K_x > 0$.

3.2. Double-cage formulation

Unlike the single-cage problem, in the double-cage problem, there is no simple expression for the slip at the point of the maximum torque. Then, the condition of the maximum torque must be imposed with Eq. (6):

$$\frac{dT(S_M)}{dS} = 0 \tag{6}$$

The inner cage has always a greater leakage flux than the outer cage; hence, the inequality $X_{1d} > X_{2d}$ must be respected. Also, the outer cage resistance can be over ten times greater than the inner cage resistance; hence, $R_2 > R_1$.

In this model, the problem formulation uses the five pieces of the manufacturer data P_{mFL}, Q_{FL}, T_M, T_{ST} and I_{ST} to find the seven double cage parameters (R_S, R_1, R_2, X_m, X_{Sd}, X_{1d} and X_{2d}). This purpose can be obtained by solving the nonlinear equation in the form of $F(X) = 0$ as follows:

$$X = R_1,\ R_2,\ X_m,\ X_{sd},\ X_{1d},\ S_M \quad F = f_1,\ f_2,\ f_3,\ f_4,\ f_5,\ f_6$$

$$\begin{aligned} f_1(X) &= P_{mFL} - Pm(S_{FL}) = 0 \\ f_2(X) &= Q_{FL} - Q(S_{FL}) = 0 \\ f_3(X) &= T_M - T(S_M) = 0 \\ f_4(X) &= I_{ST} - I(S_M = 1) = 0 \\ f_5(X) &= T_{ST} - T(S_M = 1) = 0 \\ f_6(X) &= \tfrac{dT(S_M)}{dS} = 0 \end{aligned} \tag{7}$$

Table 3 Optimal architecture and specification of the best proposed ANFIS models.

Specification	ANFIS (Single-cage)			
	R_s	R_r	X_m	X_{sd}
Type	Sugeno	Sugeno	Sugeno	Sugeno
Inputs/outputs	7/1	7/1	7/1	7/1
No. of membership functions for each input	16	10	16	11
No. of output membership functions	16	10	16	11
Input membership function type	Gaussian	Gaussian	Gaussian	Gaussian
Output membership function type	Linear	Linear	Linear	Linear
No. of fuzzy rules	16	10	16	11
No. of nonlinear parameters	112	70	112	77
No. of linear parameters	128	80	128	88
No. of epochs	150	250	200	100

	ANFIS (Double-cage)					
	R_s	R_1	R_2	X_m	X_{sd}	X_{1d}
Type	Sugeno	Sugeno	Sugeno	Sugeno	Sugeno	Sugeno
Inputs/outputs	7/1	7/1	7/1	7/1	7/1	7/1
No. of membership functions for each input	10	16	14	10	12	8
No. of output membership functions	10	16	14	10	12	8
Input membership function type	Gaussian	Gaussian	Gaussian	Gaussian	Gaussian	Gaussian
Output membership function type	Linear	Linear	Linear	Linear	Linear	Linear
No. of fuzzy rules	10	16	14	10	12	8
No. of nonlinear parameters	80	448	392	280	336	224
No. of linear parameters	280	128	112	80	96	64
No. of epochs	150	300	250	150	350	250

Table 4 Comparison between the experimental and predicted results for the Single-cage motor.

Data	Experimental				ANFIS model				ANN model			
	R_s	R_r	X_m	X_{sd}	R_s	R_r	X_m	X_{sd}	R_s	R_r	X_m	X_{sd}
Training	0.0036	0.0071	2.3801	0.0824	0.0036	0.0071	2.3798	0.0824	0.0039	0.0078	2.3808	0.0853
	0.0046	0.0092	1.7943	0.0865	0.0046	0.0092	1.7943	0.0865	0.0049	0.0097	1.7949	0.0813
	0.0041	0.0083	2.4236	0.0851	0.0041	0.0083	2.4237	0.0851	0.0038	0.0076	2.4245	0.0823
	0.0039	0.0078	1.4423	0.0747	0.0039	0.0078	1.4426	0.0747	0.0042	0.0084	1.4429	0.0796
	0.0035	0.0071	2.4082	0.0855	0.0034	0.0071	2.4071	0.0855	0.0036	0.0071	2.4081	0.0854
	0.0038	0.0076	2.2378	0.085	0.0038	0.0076	2.2378	0.085	0.0055	0.011	2.2332	0.0812
	0.0027	0.0054	2.1294	0.0772	0.0027	0.0054	2.131	0.0773	0.0056	0.0112	2.1295	0.0813
	0.0058	0.0116	2.1573	0.0835	0.0058	0.0116	2.1573	0.0835	0.0055	0.0111	2.1695	0.0813
	0.0052	0.0104	2.3228	0.0944	0.0052	0.0104	2.3228	0.0944	0.0057	0.0114	2.3241	0.0809
	0.0055	0.0111	1.6728	0.096	0.0055	0.0111	1.6728	0.0962	0.0085	0.017	1.6684	0.0806
	0.0073	0.0147	1.9975	0.0716	0.0073	0.0147	1.9975	0.0716	0.0062	0.0123	1.9857	0.0813
	0.0087	0.0174	2.3497	0.0819	0.0087	0.0174	2.3498	0.0819	0.0058	0.0115	2.3495	0.0808
	0.0115	0.0229	1.6808	0.0661	0.0115	0.0229	1.6808	0.0661	0.0083	0.0166	1.69	0.0807
	0.0131	0.0263	3.1806	0.0741	0.0130	0.0263	3.1804	0.0741	0.0137	0.0275	3.1808	0.0749
	0.0082	0.0163	2.5856	0.0719	0.0082	0.0163	2.5857	0.0719	0.0072	0.0145	2.5841	0.0796
	0.0155	0.031	1.056	0.0788	0.0155	0.0312	1.0562	0.0788	0.0153	0.0305	1.0555	0.0775
Testing	0.004	0.008	1.9026	0.076	0.004279	0.00786	1.9252	0.0759	0.0042	0.0083	2.0491	0.0835
	0.0042	0.0083	2.1209	0.0763	0.004213	0.00771	2.1414	0.0757	0.0056	0.0112	2.1274	0.0813
	0.0067	0.0134	1.7594	0.0918	0.006496	0.01327	1.8643	0.0927	0.0082	0.0164	1.7028	0.0808
	0.0104	0.0207	1.2526	0.0723	0.012203	0.01818	1.2385	0.0738	0.0144	0.0288	1.1232	0.0782

4. Artificial neural network and adaptive neuro-fuzzy inference system

4.1. Artificial neural network

An ANN is a system based on the operation of the biological neural networks. Multi-layer perceptron (MLP) networks [21,22] are the most widely used neural networks that consist of a great number of processing elements called neurons. An MLP network has at least three layers commonly named as the input layer, hidden layer and the output layer as shown in Fig. 3.

Each layer of the MLP networks has its own number of neurons. The input to the node d in the hidden layer is given by the following:

$$\rho_d = a_d + \sum_{k=1}^{i}(X_k \cdot w_{kd}) \quad d = 1, 2, \ldots, n \tag{8}$$

where X is the inputs, n is the number of neurons in hidden layer, i is the number of neurons in the input layer, a is the bias term and w is the weighting factor [21,22]. The output from dth neuron of the hidden layer is given by the following:

$$\theta_d = f(\rho_d) \tag{9}$$

where f is the activation function of the hidden layer.

The output of the cth neuron in the output layer is given by the following:

$$Y_c = b_c + \sum_{k=1}^{i}(\theta_k \cdot w_{kc}) \quad c = 1, 2, \ldots, m \tag{10}$$

where b is the bias term, w is the weighting factor, m is the number of neurons in the output layer, and i is the number of neurons in the hidden layer.

4.2. Adaptive neuro-fuzzy inference system

ANFIS is a multilayer feed-forward (FF) network, which permits the application of fuzzy logic (FL) together with ANN. Without loss of generality, we assume that the fuzzy inference system (FIS) has two inputs (x, y) and one output (f). To present the ANFIS architecture, two fuzzy if-then rules based on a first-order Sugeno FIS are considered [23,24]:

If x is A_1 and y is B_1, then $f_1 = p_1x + q_1y + r_1$
If x is A_2 and y is B_2, then $f_2 = p_2x + q_2y + r_2$

An ANFIS structure is shown in Fig. 4.

The layers of this structure are defined as follows:

Layer 1: Each node of this layer generates the membership grades of an input variable with the node functions described as follows:

$$O_{1,i} = \mu_{Ai}(x) \quad i = 1, 2 \tag{11}$$

$$O_{1,i} = \mu_{Bi-2}(x) \quad i = 3, 4 \tag{12}$$

where i is the membership grade of a fuzzy set (A_1, B_1, A_2, B_2) and $O_{l,i}$ is the output of the node i in layer l.

Layer 2: The output node in this layer products all incoming signals as follows:

$$O_{2,i} = w_i = \mu_{Ai}(x) \times \mu_{Bi}(x), \quad i = 1, 2 \tag{13}$$

Layer 3: The nodes of the Layer 3 calculate the ratio of the rule's firing strength relative to the sum of all rule's firing strengths given by the following:

$$O_{3,i} = \bar{w}_i = \frac{w_i}{w_1 + w_2}, \quad i = 1, 2 \tag{14}$$

Layer 4: All nodes in the layer 4 are the adaptive nodes with a node output:

Table 5 Comparison between the experimental and predicted results for the Double-cage motor.

Data	Experimental						ANFIS model					
	R_s	R_1	R_2	X_m	X_{sd}	X_{1d}	R_s	R_1	R_2	X_m	X_{sd}	X_{1d}
Training	0.0038	0.0077	0.1314	2.4021	0.0579	0.1158	0.00380	0.0077	0.1313	2.4023	0.0578	0.1158
	0.0054	0.0107	0.0741	1.8144	0.063	0.1261	0.0054	0.0106	0.0740	1.81456	0.0629	0.126
	0.0046	0.0093	0.09	2.442	0.0621	0.1243	0.0045	0.0092	0.089	2.441	0.06211	0.12430
	0.0048	0.0097	0.0553	1.4611	0.0536	0.1073	0.00479	0.00970	0.05530	1.46115	0.05359	0.10729
	0.0039	0.0078	0.1083	2.4351	0.0547	0.1094	0.00389	0.0077	0.1081	2.4349	0.0546	0.10937
	0.0043	0.0086	0.0821	2.261	0.0586	0.1172	0.00429	0.00859	0.0820	2.2616	0.0585	0.1172
	0.003	0.006	0.0603	2.1472	0.0591	0.1182	0.00299	0.0060	0.06038	2.14676	0.05900	0.11808
	0.0071	0.0143	0.0784	2.1727	0.0612	0.1224	0.00709	0.01429	0.07835	2.17268	0.06121	0.1225
	0.0061	0.0122	0.0883	2.3514	0.0657	0.1313	0.00609	0.01219	0.08830	2.35143	0.0656	0.13137
	0.0069	0.0139	0.0844	1.7001	0.0637	0.1274	0.00689	0.01389	0.08438	1.70024	0.0637	0.12738
	0.0091	0.0182	0.1098	2.0088	0.0567	0.1134	0.00909	0.01820	0.10973	2.0096	0.05670	0.11338
	0.0104	0.0209	0.161	2.3576	0.063	0.1259	0.01039	0.02086	0.1609	2.3575	0.0630	0.12566
	0.0187	0.0375	0.0988	1.6559	0.0518	0.1036	0.0187	0.0375	0.0988	1.6560	0.0518	0.1035
	0.023	0.046	0.1225	3.0787	0.0602	0.1203	0.0230	0.0459	0.1225	3.0785	0.0602	0.1203
	0.0106	0.0211	0.1295	2.5947	0.0598	0.1196	0.0105	0.0210	0.1295	2.5940	0.0599	0.1196
	0.0244	0.0489	0.1644	1.0415	0.0655	0.1309	0.0243	0.0496	0.1641	1.0414	0.0650	0.1301
Testing	0.0046	0.0093	0.062	1.9158	0.0602	0.1205	0.00466	0.00891	0.06353	1.81307	0.05953	0.11171
	0.0046	0.0093	0.1083	2.1405	0.0529	0.1058	0.00458	0.00933	0.141676	2.263121	0.055684	0.104410
	0.0084	0.0168	0.0848	1.7804	0.0637	0.1274	0.006810	0.013306	0.083921	1.695380	0.063752	0.127092
	0.0125	0.025	0.1947	1.2665	0.0497	0.0995	0.012539	0.025037	0.171490	1.271106	0.050314	0.108538

	ANN model					
Training	R_s	R_1	R_2	X_m	X_{sd}	X_{1d}
	0.00501	0.0100	0.1306	2.40225	0.0603	0.12070
	0.00511	0.0102	0.0743	1.8144	0.0637	0.12746
	0.0022	0.0046	0.0913	2.4419	0.0629	0.1260
	0.00583	0.0117	0.0542	1.4611	0.0539	0.1080
	0.0029	0.00582	0.1013	2.4353	0.0570	0.1141
	0.00415	0.0083	0.0902	2.2605	0.0581	0.1163
	0.00281	0.00566	0.0606	2.14715	0.0565	0.11322
	0.0044	0.0089	0.0737	2.1726	0.0596	0.1193
	0.007577	0.01527	0.0880	2.3513	0.0645	0.1290
	0.0108	0.0216	0.0824	1.7002	0.0622	0.1244
	0.0080	0.0160	0.1064	2.0088	0.0565	0.113
	0.0106	0.0213	0.1608	2.3576	0.0605	0.1210
	0.0124	0.0250	0.1004	1.6556	0.0586	0.1172
	0.0225	0.0451	0.1228	3.0788	0.0605	0.1209
	0.0123	0.0246	0.1280	2.5947	0.0587	0.1174
	0.0238	0.0478	0.1646	1.0415	0.0656	0.1312
Testing	0.0064	0.0129	0.0626	1.9158	0.0590	0.1180
	0.0060	0.0122	0.1161	2.1405	0.0549	0.109
	0.0098	0.0197	0.0857	1.7805	0.0613	0.122
	0.0129	0.0260	0.193	1.2662	0.0478	0.095

$$O_{4,i} = \bar{w}_i f_i = \bar{w}_i(p_i x + q_i y + r_i), \quad i = 1, 2 \tag{15}$$

where $\bar{w}_i$ is a normalized firing strength and p_i, q_i and r_i are called the consequent parameters.

Layer 5: Every node in layer 5 computes the overall output as the summation of all incoming signals as follows:

$$O_{5,i} = \sum_{i=1}^{2} \bar{w}_i f_i = \frac{w_1 f_1 + w_2 f_2}{w_1 + w_2} \tag{16}$$

4.3. Developing the proposed models

To develop the proposed models, the experimental data are used. The experimental data are calculated based on a numerical method from the manufacturer's measurements, which are shown in Table 1 [3,8]. The input parameters of the models are $P(KW)$, $\cos(\rho FL)$, T_m/T_{FL}, T_{ST}/T_{FL}, I_{ST}/I_{FL}, $\omega_{FL}(rpm)$ and η_{FL}. The output parameters for the Single-cage induction motor model are R_S, R_r, X_m and X_{Sd}. Also, for the Double-cage induction motor model the output parameters are R_S,

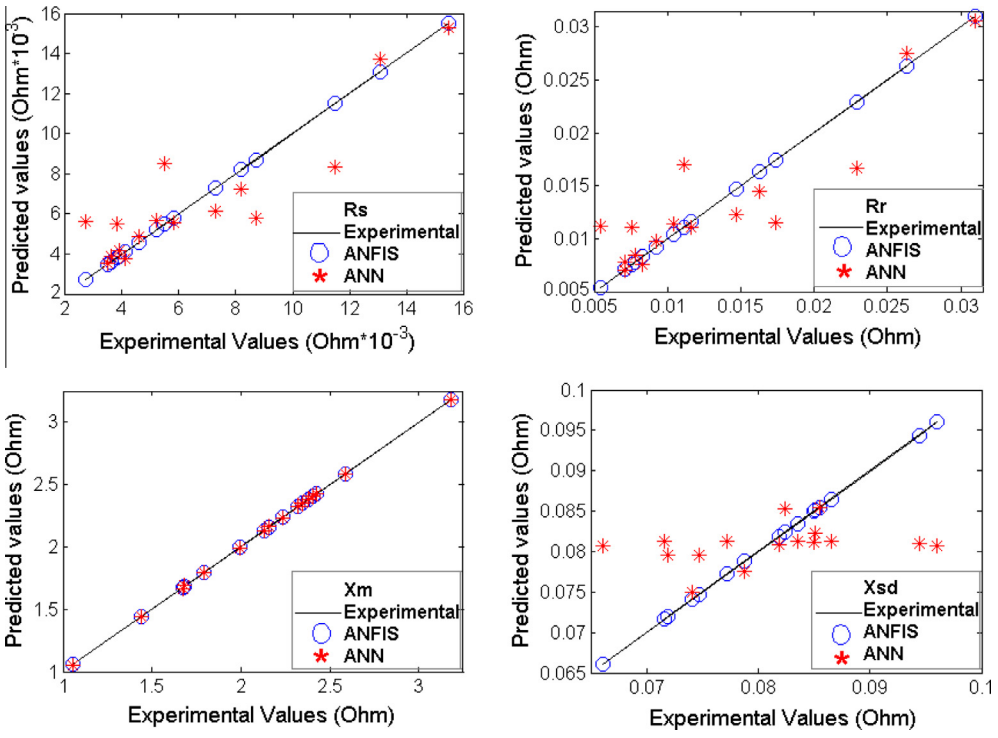

Figure 6 Comparison of the experimental and predicted results for training data (Single-cage motor).

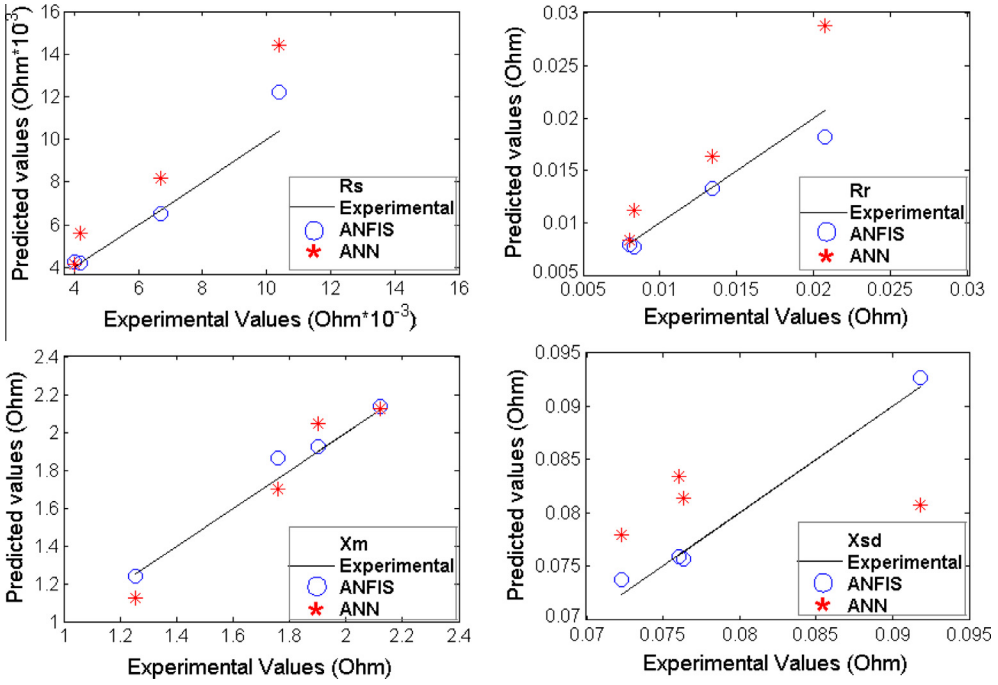

Figure 7 Comparison of the experimental and predicted results for testing data (Single-cage motor).

R_1, R_2, X_m, X_{Sd} and X_{1d}. The experimental data are divided into two sets for the training and testing the networks, where, 80% of the experimental data are used to train the networks, and the rest (20%) are used to test the accuracy of the trained models. In this study, different ANN and ANFIS structures (i.e., the networks with the different number of hidden layers and neurons in each hidden layer for the ANN models) are tested and optimized to obtain the best structures. Also we tested many different ANFIS structures to obtain the best ANFIS configuration.

The training (the greater data set) and testing data are selected randomly from the experimental data. At the first,

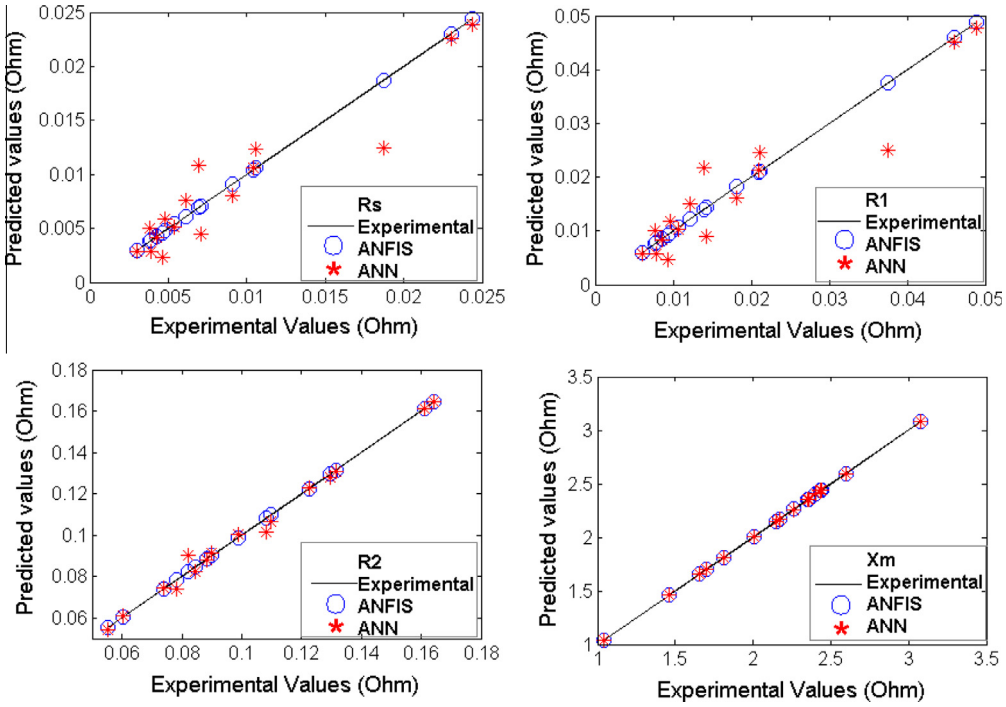

Figure 8 Comparison of the experimental and predicted results for training data (Double-cage motor).

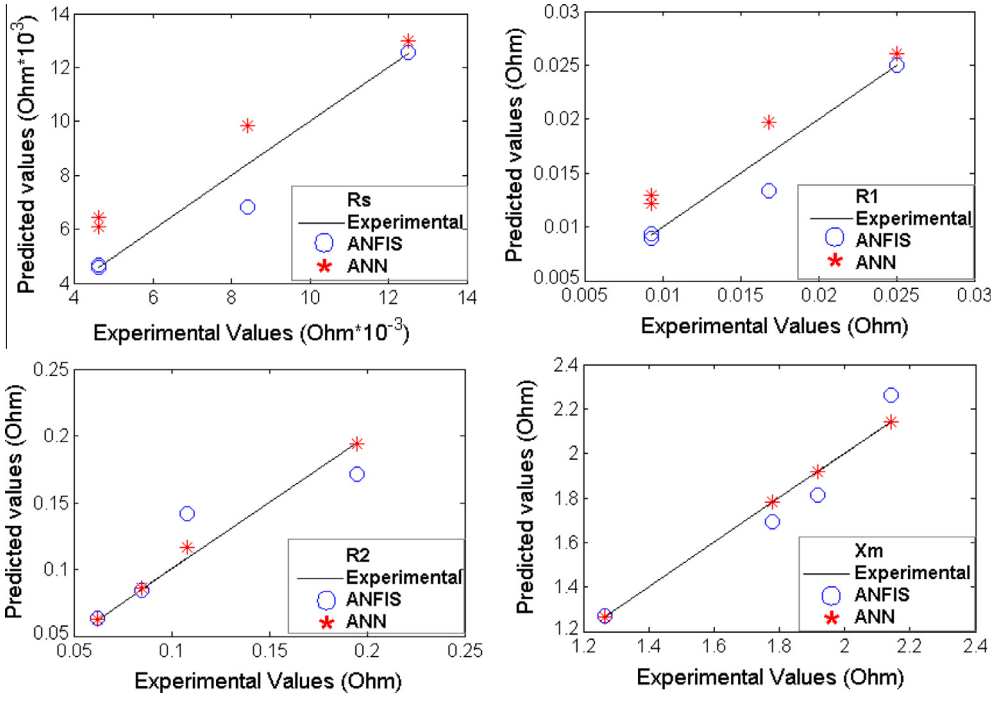

Figure 9 Comparison of the experimental and predicted results for testing data (Double-cage motor).

the training data are used to develop the different ANN and ANFIS structures (the training process). Then, the testing data set, which is unknown for the developed (trained) network is used to test the accuracy of the trained network. For training the ANN and ANFIS models, a computer program has been developed by using MATLAB 7.0.4 software. The training process algorithm to obtain the best ANN and ANFIS models is shown in Fig. 5. The obtained optimal architectures of the ANN and ANFIS models are shown in Tables 2 and 3, respectively.

5. Simulation results

In order to examine the performance of the proposed ANN and ANFIS models, the obtained results are compared with

Table 6 The obtained errors for the proposed ANN and ANFIS models.

Data	Model	Output	Network							
			ANFIS				ANN(MLP)			
			MAE	RMSE	CF	MRE%	MAE	RMSE	CF	MRE%
Training	Single-cage	R_s	3.98e−07	6.58e−07	0.999999	0.008	0.0011	0.0016	0.89590	21.70
		R_r	7.51e−07	1.47e−06	0.999999	0.008	0.0023	0.0032	0.89720	21.72
		X_m	0.0002	0.0004	0.999999	0.010	0.0030	0.0051	0.99990	0.156
		X_{sd}	4.97e−06	1.61e−05	0.999999	0.006	0.0056	0.0074	0.32490	7.040
	Double-cage	R_s	2.32e−06	3.35e−06	0.999999	0.039	0.0015	0.0021	0.945548	20.62
		R_1	7.1e−06	1.22e−05	0.999999	0.044	0.0030	0.0043	0.945264	20.33
		R_2	2.77e−05	4.64e−05	0.999998	0.030	0.0020	0.0031	0.995043	2.271
		X_m	0.00027	0.00041	0.999999	0.012	0.0001	0.0001	0.999999	0.004
		X_{sd}	2.01e−05	3.52e−05	0.999968	0.034	0.0015	0.0022	0.832689	2.707
		X_{1d}	4.11e−05	7.53e−05	0.999950	0.033	0.003	0.0044	0.832595	2.689
Testing	Single-cage	R_s	0.0005	0.0009	0.989960	6.916	0.0017	0.0022	0.992300	24.60
		R_r	0.0008	0.0012	0.993090	5.512	0.0035	0.0045	0.991100	25.21
		X_m	0.0404	0.0550	0.992401	2.308	0.0848	0.1018	0.982410	5.393
		X_{sd}	0.0007	0.0009	0.994510	0.988	0.0073	0.0076	0.152300	9.071
	Double-cage	R_s	0.00042	0.0007	0.976761	5.271	0.00131	0.00140	0.997670	23.376
		R_1	0.00098	0.0017	0.974184	6.350	0.00262	0.00279	0.997447	22.958
		R_2	0.0147	0.0203	0.917492	11.561	0.00263	0.00398	0.997765	2.47617
		X_m	0.0787	0.0906	0.969406	4.0574	8.53e−05	9.42e−05	0.999999	0.00530
		X_{sd}	0.0010	0.0014	0.977243	1.9205	0.00186	0.00191	0.951729	3.32299
		X_{1d}	0.0048	0.0063	0.825044	4.482	0.00376	0.00385	0.951045	3.35086

Table 7 The calculated torque, power and power factor for the both proposed ANN and ANFIS models.

Model	ANN system					ANFIS system				
	T_M (Nm)	T_{ST} (Nm)	T_{FL} (Nm)	P_{FL} (KW)	Cosρ_{FL}	T_M (Nm)	T_{ST} (Nm)	T_{FL} (Nm)	P_{FL} (KW)	Cosρ_{FL}
Single-cage	254.45	215.60	97.12	31.84	0.871	261.24	223.23	97.48	32.95	0.875
Double-cage	257.13	216.71	97.18	31.98	0.872	262.25	222.86	97.49	32.96	0.878

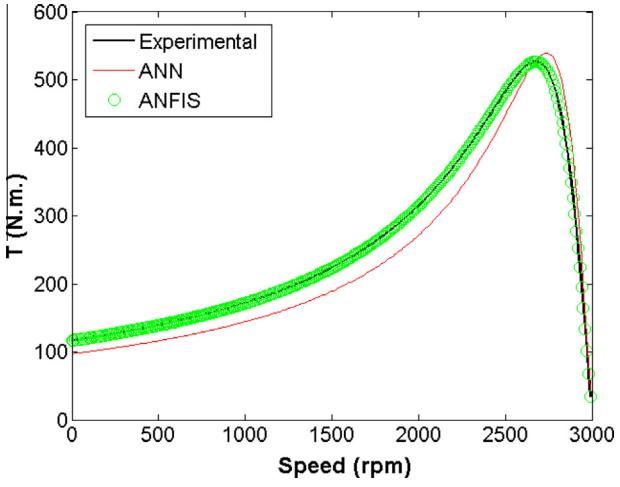

Figure 10 The torque-speed curve for the single-cage motor using the experimental and the proposed ANN and ANFIS models.

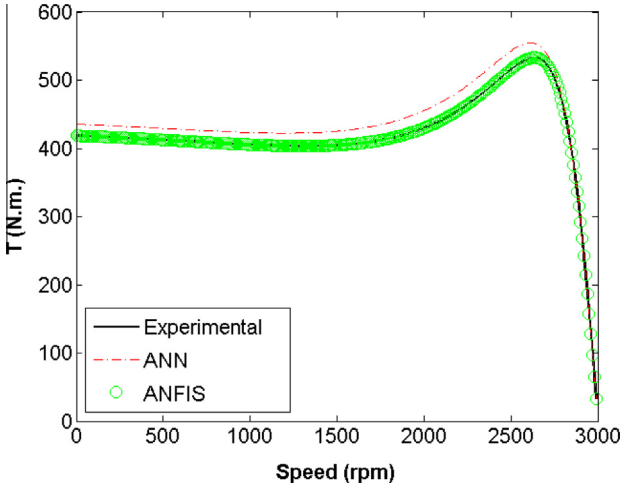

Figure 11 The torque-speed curve for the double-cage motor using the experimental and the proposed ANN and ANFIS models.

the known results. Tables 4, 5 and Figs. 6–9 compare the results obtained by the proposed ANN and ANFIS models with the experimental data for the training and testing data. The parameters in Tables 4 and 5 are in PU. The real values of the parameters can be calculated from multiplying the impedance base in PU values of the parameters, where the impedance base is $Z_b = U^2/P$, where U is the rated line voltage and P is the rated mechanical power.

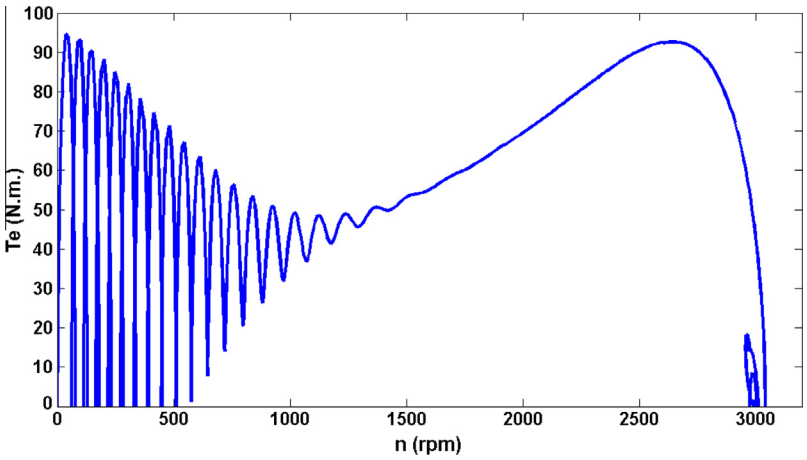

Figure 12 Dynamic behavior of a 11 kW induction motor (torque versus speed).

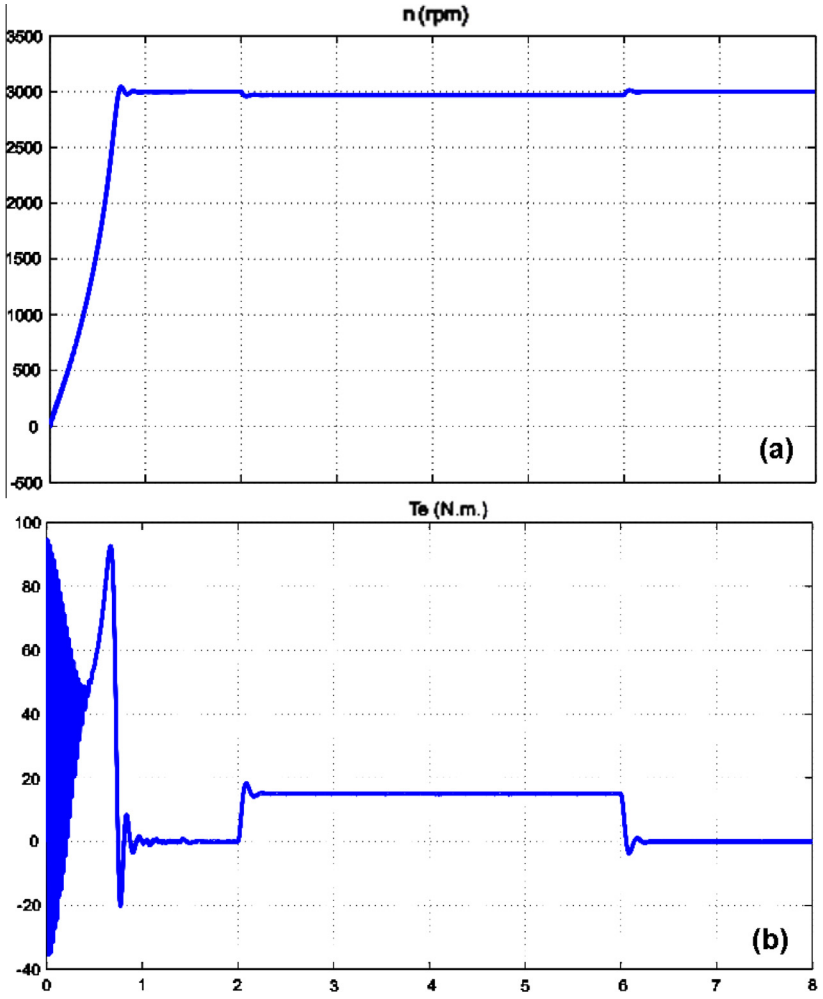

Figure 13 Dynamic behavior of a 11 kW induction motor: (a) speed versus time, (b) torque versus time.

To have more precise investigation into the proposed ANN and ANFIS models, a regression analysis of the both experimental and predicted values is performed in Figs. 6–9. The adequacy of the proposed ANN and ANFIS models can be verified using the correlation factor (CF) $0 \leqslant CF \leqslant 1$. The CF is calculated by the following:

$$CF = 1 - \left[\frac{\sum_{i=1}^{N}[X_i(Exp) - X_i(pred)]^2}{\sum_{i=1}^{N}[X_i(Exp)]^2}\right] \tag{17}$$

where N is the number of data and '$X(Exp)$' and '$X(pred)$' stand for the experimental and predicted (ANN or ANFIS)

values, respectively. As shown in Figs. 6–9, there is a good correlation between the proposed models and the experimental values for the both Single-cage and Double-cage motors.

Table 6 shows the obtained errors for the proposed ANN and ANFIS models, where the mean absolute error (MAE), the root mean square error (RMSE) and the mean relative error percentage (MRE%) of the proposed models are calculated by the following:

$$\mathrm{MAE} = \frac{1}{N}\sum_{i=1}^{N}|X_i(Exp) - X_i(pred)| \tag{18}$$

$$\mathrm{RMSE} = \left[\frac{\sum_{i=1}^{N}[X_i(Exp) - X_i(pred)]^2}{N}\right]^{0.5} \tag{19}$$

$$\mathrm{MRE}\ \% = 100 \times \frac{1}{N}\sum_{i=1}^{N}\left|\frac{X_i(Exp) - X_i(pred)}{X_i(Exp)}\right| \tag{20}$$

where N is the number of data and '$X(Exp)$' and '$X(pred)$' stand for the experimental and predicted (ANN or ANFIS) values, respectively.

From Tables 4–6 and Figs. 6–9, it is clear that the predicted outputs by the proposed ANFIS and ANN models are close to the experimental results, which shows the applicability of ANN and ANFIS as the accurate and reliable models for the modeling of the Squirrel-cage type induction motors. Also, from the obtained results it can be seen that the proposed ANFIS models are more accurate than the proposed ANN models. The proposed ANFIS model is more accurate than the proposed ANN model. The ANFIS model could significantly reduce the average (the training and testing in the Single-cage motor) MRE% to less than 1.97% in comparison with the ANN model, which has the average (training and testing) MRE% less than 14.37%. In this case, the average CF for both training and testing data is greater than 0.99623 and 0.7795 for the proposed ANFIS and ANN models, respectively. For the Double-cage motor, the ANFIS model could significantly reduce the average (the training and testing) MRE% to less than 2.82% in comparison with the ANN model, which has the average (training and testing) MRE% less than 9.68%. In this case, the average CF for the both training and testing data is greater than 0.97000 and 0.95380 for the proposed ANFIS and ANN models, respectively. Also, the training process of the ANFIS model to reach the convergence is faster. In comparison with the proposed ANN models, the time needed for the training the ANFIS models was less than the required time to design the proposed ANN models. The obtained set of parameters for the used motors can be effectively used to calculate the torque, power and power factor accurately. To show it, one of the used induction motors (30 kW) is selected to calculate the maximum torque T_M, the starting torque T_{ST}, the full load torque T_{FL}, the full load active electrical power P_{FL} and the full load power factor $\mathrm{Cos}\rho_{FL}$ [8]. The calculated results for both proposed ANN and ANFIS models are shown in Table 7.

The torque-speed behaviors of the single-cage and double-cage induction motors are shown in Figs. 10 and 11, respectively. In these figures, a comparison has been done between the experimental and the ANN and ANFIS results (with a rated power 90 kW and a line voltage 400 V). From Figs. 10 and 11 it is clear that the proposed ANFIS model is more accurate than the proposed ANN model. Also, it can be seen that, the single-cage induction motor has a lower starting torque than the double-cage induction motor. Fig. 12 shows the dynamic behavior (Torque versus Speed) of a 11 kW induction motor during a variation (step) in the load torque from $t = 2$ s to $t = 6$ s. In Fig. 13 the dynamic behavior (Torque and Speed versus Time) of a 11 kW induction motor is shown.

6. Conclusion

This paper proposes a new method for the parameters estimation of the squirrel-cage induction motors (in the single-cage and double-cage models). To predict and estimate these parameters, the ANN and ANFIS models are used with the minimum error. For developing the proposed models, the experimental data of 20 induction motors with the different power are used. The comparison shows that not only the results of both ANN and ANFIS models are in good agreement with the experimental data, but also the ANFIS models are more accurate than the ANN models.

References

[1] H. Arabaci, O. Bilgin, Squirrel cage of induction motors simulation via Simulink, Int. J. Model Opt. 2 (2012) 324–327.

[2] F. Corcoles, J. Pedra, M. Salichs, L. Sainz, Analysis of the induction machine parameter identification, IEEE Trans. Energy Convers. 17 (2) (2002) 183–190.

[3] L. Monjo, H.K. Jafari, F. Corcoles, J. Pedra, Squirrel-cage induction motor parameter estimation using a variable frequency test, IEEE Trans. Energy Convers. 30 (2) (2014) 550–557.

[4] L. Monjo, F. Corcoles, J. Pedra, Saturation effects on torque and current slip curves of squirrel-cage induction motors, IEEE Trans. Energy Convers. 28 (1) (2013) 243–254.

[5] L. Monjo, F. Corcoles, J. Pedra, Parameter estimation of squirrel-cage motors with parasitic torques in the torque-slip curve, IET Electr. Power Appl. 95 (2015) 377–387.

[6] J. Pedra, Estimation of typical squirrel-cage induction motor parameters for dynamic performance simulation, IEE Proc.-Gener. Transm. Distrib. 153 (2) (2006) 137–146.

[7] J. Pedra, L. Sainz, F. Corcoles, Study of aggregate models for squirrel-cage induction motors, IEEE Trans. Power Syst. 20 (3) (2005) 1519–1527.

[8] J. Pedra, F. Corcoles, Estimation of induction motor double-cage model parameters from manufacturer data, IEEE Trans. Energy Convers. 19 (2) (2004) 310–317.

[9] J. Pedra, F. Corcoles, Double-cage induction motor parameters estimation from manufacturers data, IEEE Trans. Energy Convers. 19 (2) (2004) 310–317.

[10] L. Peretti, M. Zigliotto, Automatic procedure for induction motor parameter estimation at standstill, IET Electr. Power Appl. 6 (4) (2012) 214–224.

[11] H.V. Khang, A. Arkkio, Parameter estimation for a deep-bar induction motor, IET Electr. Power Appl. 6 (2) (2012) 133–142.

[12] H.K. Jafari, L. Monjo, F. Corcoles, J. Pedra, Parameter estimation of wound-rotor induction motors from transient measurement, IEEE Trans. Energy Convers. 29 (2) (2014) 300–308.

[13] H.K. Jafari, L. Monjo, F. Corcoles, J. Pedra, Using the instantaneous power of a free acceleration test for squirrel-cage motor parameters estimation, IEEE Trans. Energy Convers. 30 (3) (2015) 974–982.

[14] D. Chandra Sekhar, G.V. Marutheshwar, Modeling and direct torque control of induction motor by using hybrid control technique, ELELIJ 3 (2) (2014) 17–33.
[15] R.V. Jacomini, C.M. Rocha, J.A.T. Altuna, J.L. Azcue, C.E. Capovilla, A.J. Sguarezi, Implementation of a Neuro-Fuzzy Direct Torque and Reactive Power Control for Doubly Fed Induction Motor, Industrial Electronics Society, in: IECON 2014–40th Annual Conference of the IEEE, 2014, pp. 648–654.
[16] R. Wamkeue, D. Aquglia, M. Lakehal, P. Viarouge, Two-step method for identification of nonlinear model of induction machine, IEEE Trans. Energy Convers. 22 (4) (2007) 801–809.
[17] A. Lalami, R. Wamkeue, I. Kamwa, M. Saad, J.J. Beaudoin, Unscented kalman filter for non-linear estimation of induction machine parameters, IET Electr. Power Appl. 6 (9) (2012) 611–620.
[18] M.Z. Fortes, V.H. Ferreira, A.F. Coelho, The induction motor parameter estimation using genetic algorithm, IEEE Latin Am. Trans. 11 (5) (2013) 1273–1278.
[19] H.K. Jafari, L. Monjo, F. Corcoles, J. Pedra, Multiple-global-bets guided artificial bee colony algorithm for induction motor parameter estimation, Turkish J. Electr. Eng. Comput. Sci. 22 (1) (2014) 620–638.
[20] M.G. Gonzalez, F. Jurado, I. Perez, Shuffled frog-leaping algorithm for parameter estimation of a double-cage asynchronous machine, IET Electr. Power Appl. 6 (8) (2012) 484–490.
[21] S. Haykin, Neural Networks, A Comprehensive Foundation, second ed., Prentice Hall, Englewood Cliffs, N J, 1999, pp. 178–274 (Chapter 4).
[22] M.T. Hagan, H.B. Demuth, M.H. Beale, Neural Network Design, PWSPub. Co., Boston, MA, 1996, pp. 20–110 (Chapter 2–5).
[23] J.S.R. Jang, C.T. Sun, Neuro-fuzzy modeling and control, IEEE 83 (1995) 378–406.
[24] H. Bunke, A. Kandel, Neuro-Fuzzy Pattern Recognition, World Scientific Publishing Co. Pte. Ltd., Singapore, 2000, pp. 23–75 (Chapter 2–3).